Chapter

Wetting of Al Alloys for Hot Dipping Coating Process

Qiaoli Lin, Ran Sui and Weiyuan Yu

Abstract

Wetting phenomenon, as a basic physical process, also relates to the many material processes, such as coating process, brazing or soldering process, casting, preparation of MMCs, etc. In this chapter, the method of wetting characterization at the high temperatures was presented (especially for the metallurgical melts), also the wetting behavior and mechanism of Al alloys (4043 and 6061 alloys) on the different metallic substrates at isothermal dwelling process as well as the characteristics and formation mechanism of precursor film were discussed. Thermodynamics of segregation of solute element were also discussed, which can be predicted by the thermodynamic model. We believe the content of this chapter would be a guidance for hot dipping process based on the wetting theories.

Keywords: wettability, aluminizing, brazing, interfacial reaction, adsorption, precursor film

1. Introduction

At high temperatures, wetting of a solid (metal or ceramic) by the molten metallurgical melts is of great technological importance in a variety of metallurgical processes, e.g, hot dipping coating process, brazing process, casting process and sintering process. Each process has the different optimal wetting condition. For the hot dipping coating process, the perfect wettability of base materials by liquid metal is demanded. Two key issues for wetting at high temperatures include the spreading dynamics (wetting behavior) and the final wettability (the degree of wettability). For the former issue, it determined the technological parameters in process; for the latter issue, it would be one of the critical evaluation bases for whether the process can be carried out or not.

The description of wettability since from 1805 in Young's work [1], has been well developed, as following,

$$\cos\theta = \frac{\sigma_{sv} - \sigma_{sl}}{\sigma_{lv}} \quad (1)$$

where θ is contact angle for a liquid equilibrium with ideal solid at the point of triple line, σ_{lv}, σ_{sv} and σ_{sl} are the tension between liquid-vapor, solid-vapor and solid-liquid interfaces. The value of θ represents the degree of wettability, i.e., the better wettability and the smaller θ, also cosθ stands for the energy in a dimensionless form. The methods for obtaining θ are numerous, but for the

wetting system of metallurgical melts at high temperatures, need to consider many other factors, not just the high temperatures, metallurgical process, atmosphere, interfacial reaction, etc. Further, the characterization of wetting should pay attention to two points, one is the wetting under the quasi-ideal condition, another is the wetting in a real process which including the consideration of many other factors, such as nonequilibrium temperature field, heat input and output, physic-chemistry effect of flux on interface, etc. Due to the complexity, the method for the characterization of the wetting under the quasi-ideal condition would be elaborated in Section 2.

The coating process by using a hot dipping method, although a traditional technology with relatively high energy consumption, is also a reliable technology with high efficiency. The quality of coating directly depends on the wetting of base metal by the coating metal. The performance of coating as well as the technological parameters in the coating process is also affected by the trace addition in the alloys which may act on the solid/liquid interface and(or) the liquid/vapor interface. In this chapter, based on the effect of trace elements on the wetting behaviors and the interfacial structures, the wetting mechanism of base metals (steel, Ti6Al4V (TC4) alloy, pure Ti (TA2)) by Al alloys (4043 alloy and 6061 alloy) as well as the formation of precursor film in these systems would be presented in Section 3.

This chapter presents an overview of wetting parameters at high temperatures, wetting mechanism in the isothermal spreading, the effect of trace elements on the formation of interface and the possibility of designed interfacial structures.

2. Characterization of wetting behavior

At high temperatures, one needs to be careful in the characterization of the wetting of molten metal on the surface of materials (ceramics or metals) with relatively high melting pointing under the quasi-ideal condition.

First, the basic condition is the homogeneous temperature field for wetting should be established.

Second, the average roughness (R_a) of substrate should be obtained before wetting test. Usually, R_a for the metallic substrates after polishing and the monocrystal ceramic substrates are in the range of dozens of nanometers over a distance of 2 mm, R_a for the polycrystal ceramic substrates after polishing are in the range of hundreds of nanometers which depends on the relative density of the polycrystal ceramic substrates.

Third, due to the high sensitivity of metal to oxygen, the oxygen partial pressure in the atmosphere should be controlled, usually in a vacuum of ~10^{-4} Pa or a dried-deoxidized Ar atmosphere, the oxygen partial pressure was estimated to be lower than 10^{-14} Pa [2] in such a high vacuum, and the oxygen partial pressure was estimated to be lower than 10^{-8} Pa [2] in a dried-deoxidized Ar atmosphere.

Once the above conditions were confirmed, and then the various methods for the testing should be considered.

Several methods for the testing at room temperatures, such as sessile drop method, wetting balance method, vertical rod method, tilted plate method, capillary rise method, etc., but the sessile drop method based on the complicated calculation is usually adopted due to the good feasibility. One also should note that the sessile drop method used in more than 90% of wetting studies at high temperatures [3]. The size of drop for testing should refer to its capillary length (i.e., $2\sigma_{lv}/(\rho g)^{1/2}$, where ρ is the density of liquid and g is the acceleration due to gravity), and thus

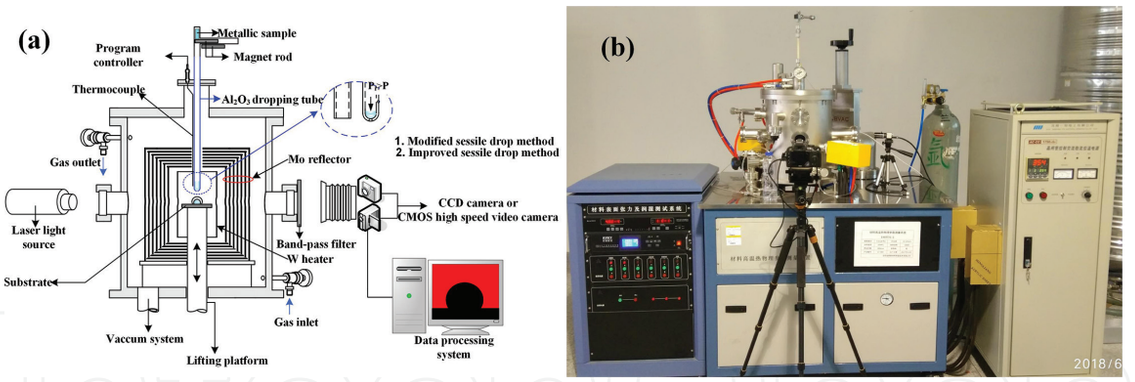

Figure 1.
(a) Schematic diagram for wetting furnace and (b) the designed wetting furnace.

a drop of volume ~5 μl with a spherical diameter of ~2 mm will be suitable for obtaining of the contact angle. Advancing contact angle is the parameter which the engineers mostly care about, and thus the study of wetting behavior used the advancing contact angle.

To acquire wetting parameters under the quasi-ideal condition, a specific wetting furnace is necessary, as be shown in **Figure 1**. The whole device mainly includes the controlled heat system, the vacuum system, the inertia gas flow system, the water-cooling system, and the image acquisition and data processing system. The details of this device were shown in **Figure 1(a)**, W, Ta or Mo was used as a heater, and two typical drop transfer modes were used, the modified sessile drop method and the improved sessile drop method.

Comparing to the traditional sessile drop method (substrate and metal were heated together), the mentioned two sessile drop methods have a distinct advantage in measurement of initial contact angle and spreading dynamics, particularly for the system with a chemical reaction at elevated temperatures.

To acquire the wetting parameters accurately, a laser backlight source (650 nm in wavelength and 10 mW in power) together with the band-pass filter is necessary for an image acquisition and data processing system. To insure the reliability of obtained data, the drop profiles were captured in two axes, as shown in **Figure 1(b)**. The typical side view of captured drop profile was shown in **Figure 2**. Before the calculation of contact angle, every pixel in the image was defined as a coordinate value (x and y coordinates), and then the program can seek the boundary between drop and backlight, and thus the pixel coordinate function of drop profile can be

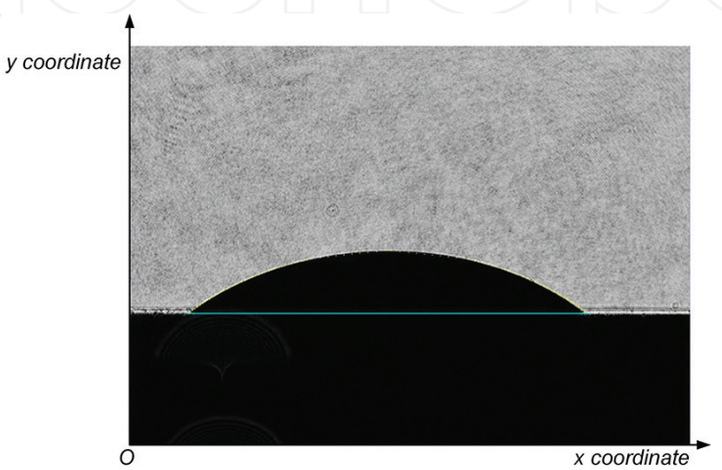

Figure 2.
Typical captured drop profile.

	Si	Fe	Cu	Mn	Mg	Zn	Ti	Al
Al 6061	0.60	0.90	—	—	0.90	0.25	0.15	Bal.
Al 4043	4.5–6.0	0.80	0.30	0.05	0.50	0.10	0.20	Bal.

Table 1.
Nominal chemical compositions of the used Al alloys (wt.%).

Steel	C	Si	Mn	P	S	Fe	
Q235	0.12–0.2	≤0.3	0.3–0.7	≤0.045	≤0.045	Bal.	
Ti alloy	Ti	Fe	Si	C	Al	V	O
TC4	Bal.	0.3	—	0.1	5.6–5.8	3.5–4.5	0.2
Pure Ti	Ti	Fe	Si	C	N	H	O
TA2	Bal.	0.3	0.15	0.1	0.05	0.015	0.2

Table 2.
Nominal chemical compositions of the used substrates (wt.%).

extracted. The function was further fitted by several models, i.e., Young-Laplace model, conic model, circle model. The choice of fitting model depends on the symmetry of captured drop profile or the contact angle. If the drop profile is almost axisymmetric, Young-Laplace model is the first choice. If the profile deviates axis symmetry, conic model is the first choice. If the contact angle is less than 5°, conic model or circle model is the first choice. Based on the results of calculation, the detailed wetting parameters can be obtained, i.e., the contact angle, the base diameter, the density, volume and surface tension of liquid.

The chemical compositions of the used materials were shown in **Tables 1** and **2**.

Based on the wetting characterization, to establish the relationship of wetting behavior and surface/interface evolution, further reveal the wetting mechanism, some necessary micro-analysis were also carried out.

3. Reactive wetting of Al alloys on metallic substrates

Trace elements in Al alloys, which may act on the surface of drop and/or the solid/liquid interface, and thus the industrial grade Al 4043 alloy and Al 6061 alloy were selected in this work which are of Si addition (~5 wt.%) and of Mg addition (~1 wt.%), respectively. The Si addition may both act on the surface of drop and solid/liquid interface, and the Mg addition may act on the surface of the drop mainly. The metallic substrates were selected as a reactive wetting system, i.e., Al/steel (low-carbon steel), Al/TC4 (Ti6Al4V) and Al/TA2 (TA2 grade pure Ti) systems.

The melting points of Al 4043 alloy and Al 6061 alloy were confirmed by DTA method (STA449-C, NETZSCH, and Germany), are 586 and 582°C, respectively, and thus the isothermal wetting experiments were carried out in a high vacuum (~10^{-4} Pa) by using improved sessile drop method at the range from 600 to 700°C.

The variations in the contact angle and the normalized contact radius (R_d/R_0, R_d is the dynamic contact radius and R_0 is the initial contact radius) with time are critical parameters for fabricating a coating by hot dipping method, were shown in **Figures 3** and **4**. **Figure 3** for Al/steel, **Figure 4(a)–(d)** for Al/TC4, **Figure 4(e)–(h)** for Al/TA2, all show the monotonic variation with time and the temperature depended final wettability. In variations of normalized contact radius with time, there are two types of variations, i.e., the linear spreading and

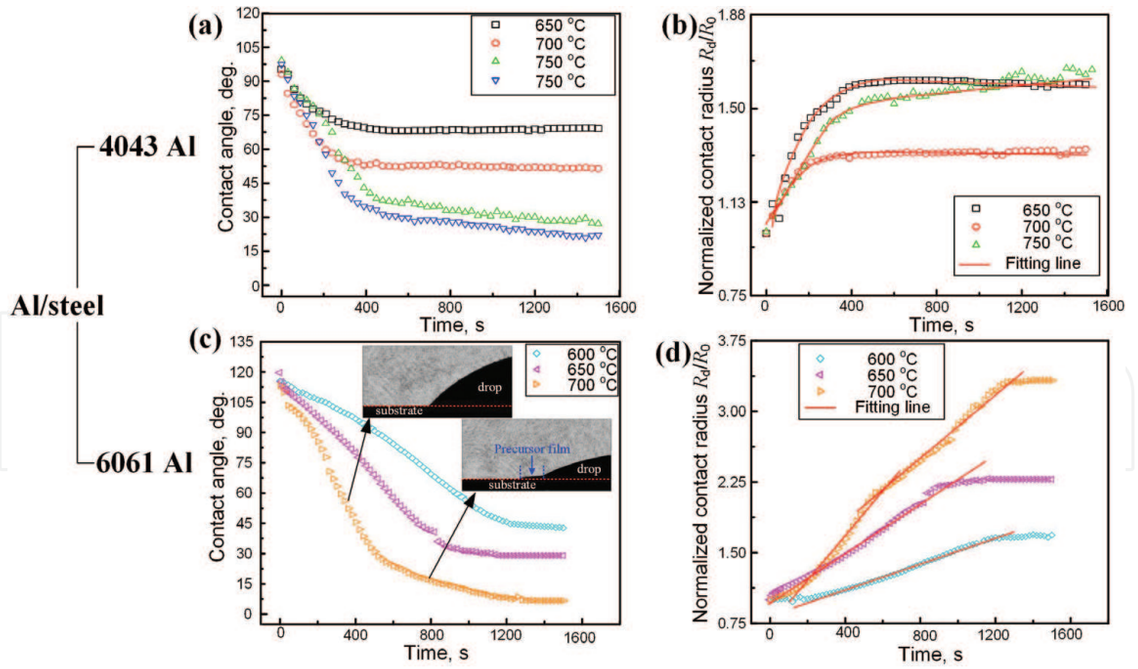

Figure 3.
Variation in contact angle and normalized contact radius with time, (a) and (b) for 4043 Al/steel, (c) and (d) for 6061 Al/TC4, respectively.

the nonlinear spreading. In Al/steel system, the variation of Al 4043 is in the nonlinear spreading, and the variation of Al 6061 is in the linear spreading; In Al/TC4 and Al/Ti systems, the variations of R_d/R_0 show that nonlinear spreading firstly, and then linear spreading. The variations of the nonlinear spreading can be described by the exponential function ($R_d/R_0 = R_f/R_0\text{-}a\exp[-(t/\tau)^m]$, where a, τ and m are the fitting parameters, R_f represents the final contact radius).

During spreading, the precursor film (diffusion bond or so called "wetting halo") was formed at the latter stage of spreading in some specific samples. As shown in **Figure 5(a)–(c)** are the top-views for the samples after isothermal wetting at 650, 700 and 750°C for Al 4043/steel, and the top-views of (a-1) to (c-1) for Al 6061/steel samples after isothermal wetting at 600, 650 and 700°C. As a consensus, the formation of the precursor film always accompanies the good final wettability, and the larger width of the precursor and the better final wettability. Therefore, the final wettability of Al 6061/steel is better than Al 4043/steel at the same experimental temperature, although the latter has some precursor film at 650 and 700°C, the width of them is very limited (~500–1000 μm). Such a congruent relationship is also suitable for the wetting of metal/ceramic systems [4]. Also, in all Al/TC4 and Al/TA2 (except for Al 6061/TA2 at 600°C which is nonwetting at the final state), the precursor film can be found at the final state after wetting, also can be seen in Hg/Ag system [5] in the study by Be'er et al. However, the formation mechanism is so different from the evaporation-condensation mechanism (suggested by de Gennes [6]) and the surface diffusion mechanism (suggested by Li et al. [7]). Further, the precursor film, in a metal/ceramic system, especially for the melt contain some concentration of the active element, is an adsorbed film. The formation of the film should satisfy some specific conditions, as we reviewed before [4].

The sectional views of interfacial structures for Al 6061/steel and Al 4043/steel samples are obviously different after isothermal wetting at the same temperature (at 650°C), as shown in **Figures 6(a)** and **7(a)**. Although two types of Fe-Al intermetallics can be found in all the samples (bottom: the continuous Fe_2Al_5 layer, upper: discontinued $FeAl_3$), the effect of trace elements on the interfacial structures is obvious. In Al 4043/steel, the addition of Si segregated at solid/liquid interface

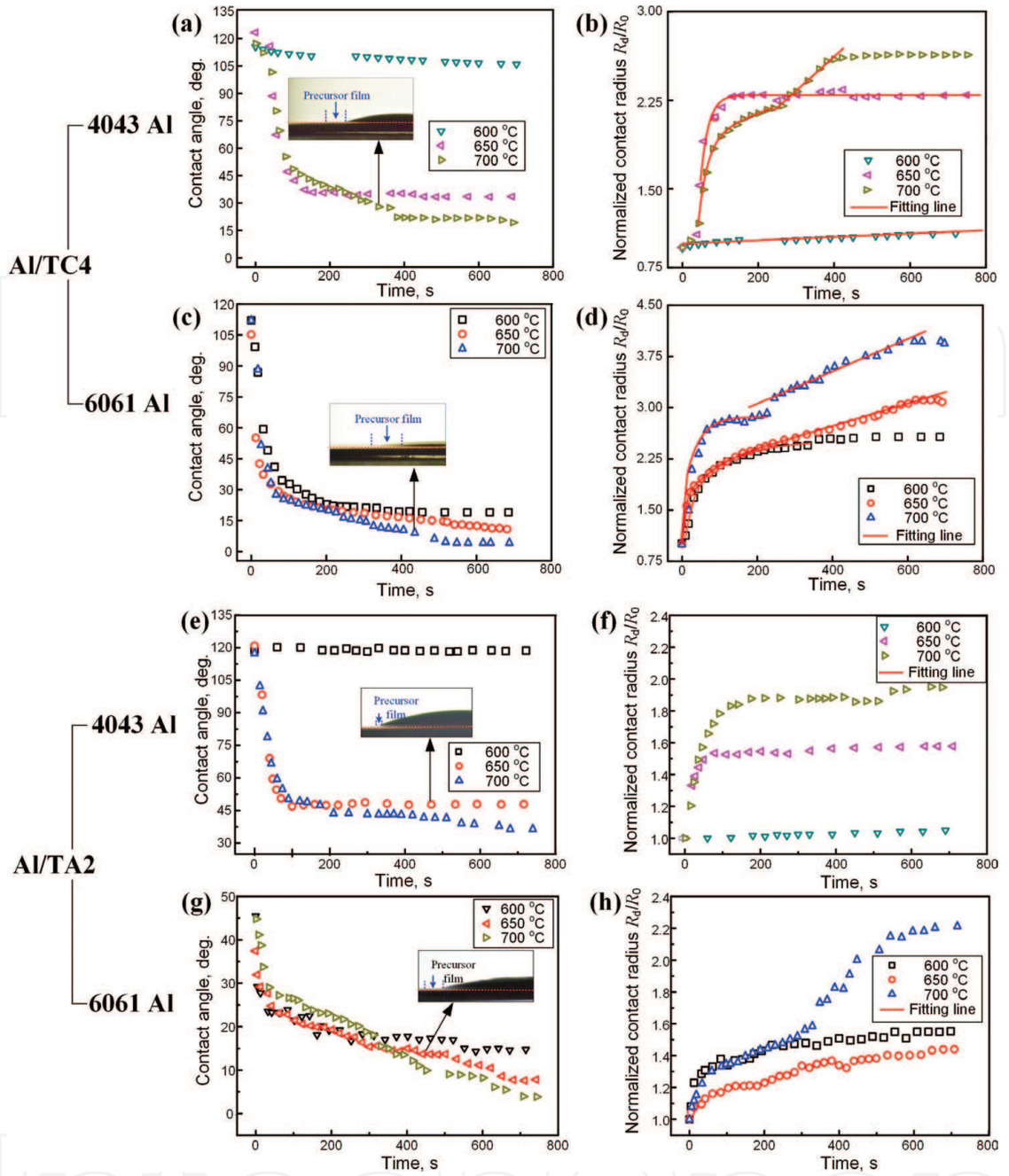

Figure 4.
Variation in contact angle and normalized contact radius with time, (a) and (b) for 4043 Al/TC4, (c) and (d) for 6061 Al/TC4, (e) and (f) for 4043 Al/TA2, (g) and (h) for 6061 Al/TA2, respectively.

which enhanced the interfacial reaction, so that the barrier of interdiffusion was established. Both Si element distribution map (**Figure 6(c)**) and the elements line distributions for the corresponding position of **Figure 6(b)** show Si is incline to segregate at solid/liquid interface rather than surface of liquid. Also, the segregation of Si induced the brittleness of the compact Fe_2Al_5 layer [8], which induced some continuous and propagating cracks. Actually, some Si was dissolved into the Fe_2Al_5 phase as a solid solution due to the Si segregation, which can be rewritten as $Fe_2(Al_{1-x}Si_x)_5$, where x is in the range of 0.0625–0.104, as reported by Gupta [9]. Comparing with Al 4043/steel, in the interface of Al 6061/steel, no Mg segregation (even no trace of Mg) can be found in the interface or the bulk of drop due to the high volatility of Mg under the vacuum condition, as shown in **Figure 7(a)–(c)**. The Fe_2Al_5 reaction layer on steel side is irregular and stretches into the steel side, which is one of the main differences from Al 4043/steel interface. Without the barrier

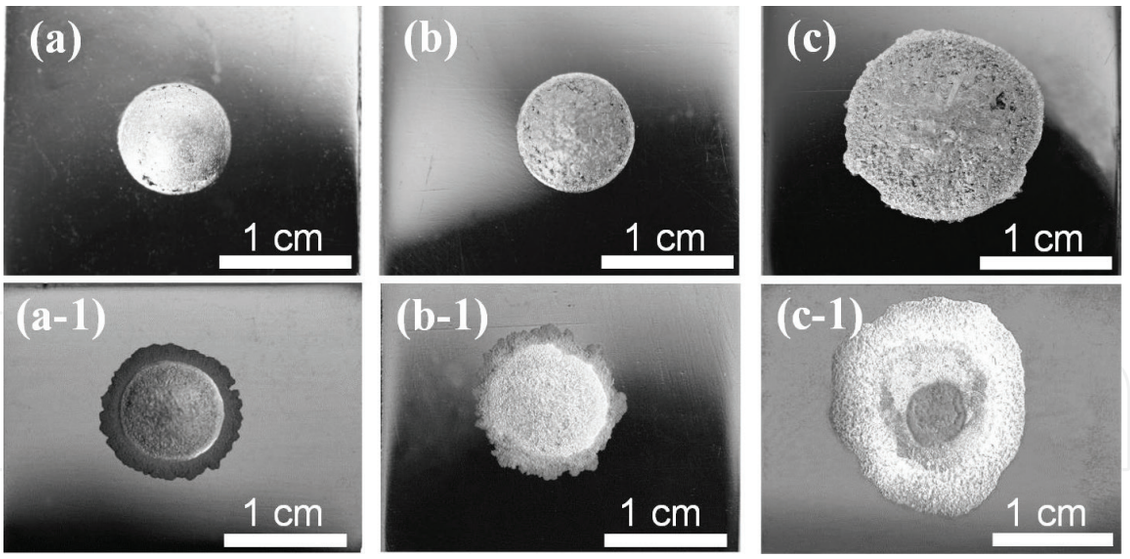

Figure 5.
Top-view of some typical sessile drop samples of Al/steel after the wetting experiments in vacuum: (a)–(c) for Al 4043 sample at 650, 700 and 750°C; (a-1)–(c-1) for Al 6061 sample at 600, 650 and 700°C.

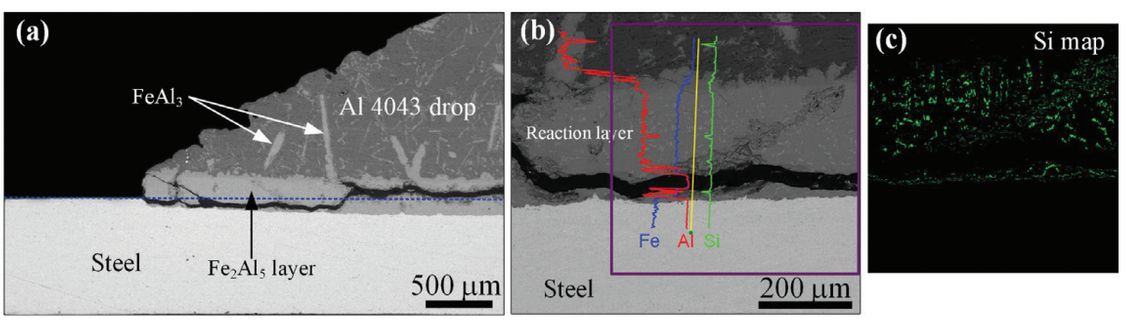

Figure 6.
Cross-sectional views of interface structures (Al 4043/steel): (a) at the close of triple line, (b) the central position at interface, (c) Si element distribution map corresponding to the purple rectangle in (b).

of interdiffusion, the grain boundary as a short-circuit diffused path, Al element prefers to diffuse into the grain boundary, and then reacted with Fe. The X-Ray micro-Diffraction (micro-XRD) pattern of the phases at the surface of the precursor film for Al 6061 sample after isothermal wetting at 700°C in **Figure 7(d)** shows the precursor film contains Fe_2Al_5, i.e., the extended reaction layer.

Understanding the reasons caused the wetting, is the benefit of further controlling the manufactured process, which is the prime concern of engineering. In a metallic system, the first obstacle for wetting is the oxide film on the surface of substrate. Protsenko et al. [10] considered the effect of the formation of intermetallic compounds in the wetting with the metallic substrate covered by oxide film. By the formation of IMC by diffusion of reacting components through the thin oxide layer, the oxide film can be disrupted and then in situ a clean surface of intermetallic for wetting can be created. Also, as suggested by Durandet et al. [11], the precipitation of Fe-Al intermetallics is so fast even the contact time of liquid Al and steel as short as 20 ms. Further, the thickness of the IMC layer in this work is larger than the oxide film (in nanoscale), and thus the precipitation of IMC may be a factor for improving wettability. However, the time for spreading cannot correspond to the fast reaction.

The dynamic of IMC precipitation should not be the limited factor for spreading. Although the nonwettable Fe—O oxide film would block wetting, a reduction reaction $2yAl + 3Fe_xO_y = yAl_2O_3 + 3xFe$ can take place based on the thermodynamic consideration [12], and then Al melts can further react with the fresh surface of Fe.

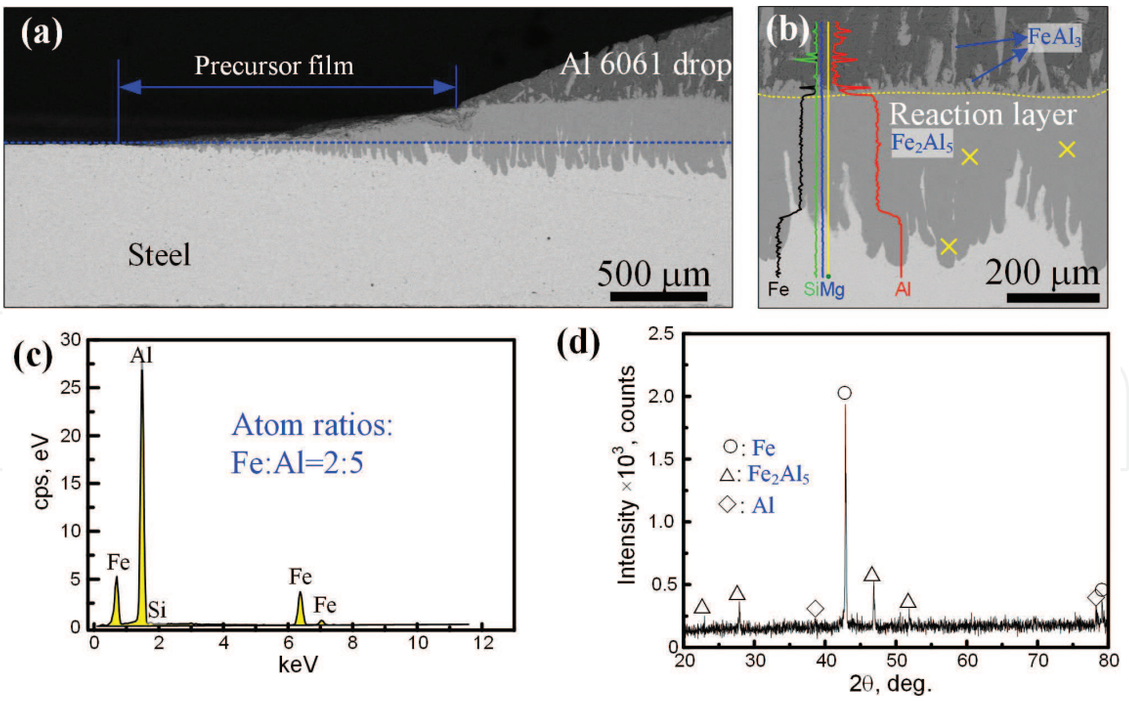

Figure 7.
Cross-sectional views of interface structures (Al 6061/steel): (a) at the close of triple line, (b) the central position at interface, (c) the typical energy spectrum for the position of yellow cross in (b) and (d) the XRD pattern for the surface of precursor film.

As known, the whole process is limited by the slowest step, and thus the reduction step may be the limited factor for spreading. In Al 6061/steel, although no trace of Mg was observed, the volatilization of Mg cannot be neglected. As suggested by Miller and Pa [13], Mg vapor as a gas flux can reduce Al_2O_3 in the brazing process of Al alloys. Here, the Fe—O oxide film also can be reduced by Mg vapor due to the more positive formation of Gibbs free energy of Fe—O compounds [12] under the same thermodynamic condition. Based on the result of microstructures, although the precursor film for Al 4043/steel also can be found, it only appears at high experimental temperature with very limited width due to the slight volatility of Al. All the interfacial structures indicate that the formation of the precursor film is related to the volatility of the active element in the specific system. However, the formation mechanism is not the evaporation-condensation mechanism. When the base metal was covered by the thin oxide film, the molten metal would infiltrate under the covered oxide film and then trigger the moving of triple line, and thus the spreading in this stage is also called secondary spreading or wetting, i.e., the formation of precursor film satisfies the subcutaneous infiltration mechanism (as proposed by Zhuang and Lugscheider [14]).

Based on the final wetting states, i.e., nonwetting and wetting states, the typical interfacial structures were selected, as shown in **Figures 8–10**. In **Figure 8(a)** and **(b)**, the precursor with width of several millimeters as well as some Al-Ti intermetallics in the precursor film can be found. The obvious precursor film in Al/TC4 and Al/TA2 (except for the Al/TC4 and Al/TA2 at 600°C which are nonwetting) has the same formation mechanism i.e., so-called "subcutaneous infiltration". The final wettability was less affected by the oxide film but was determined by the reaction products at the liquid/solid interface. As known, although some residual oxygen in the vacuum chamber could dissolve into Ti due to the high affinity of Ti to oxygen, and then inducing oxidation, however, the diffusion rate for oxygen into the interior of Ti is faster than the oxidation rate so that the oxide film would be thinned or even removed. In Al/TC4 and Al/TA2 systems, both the temperatures and the

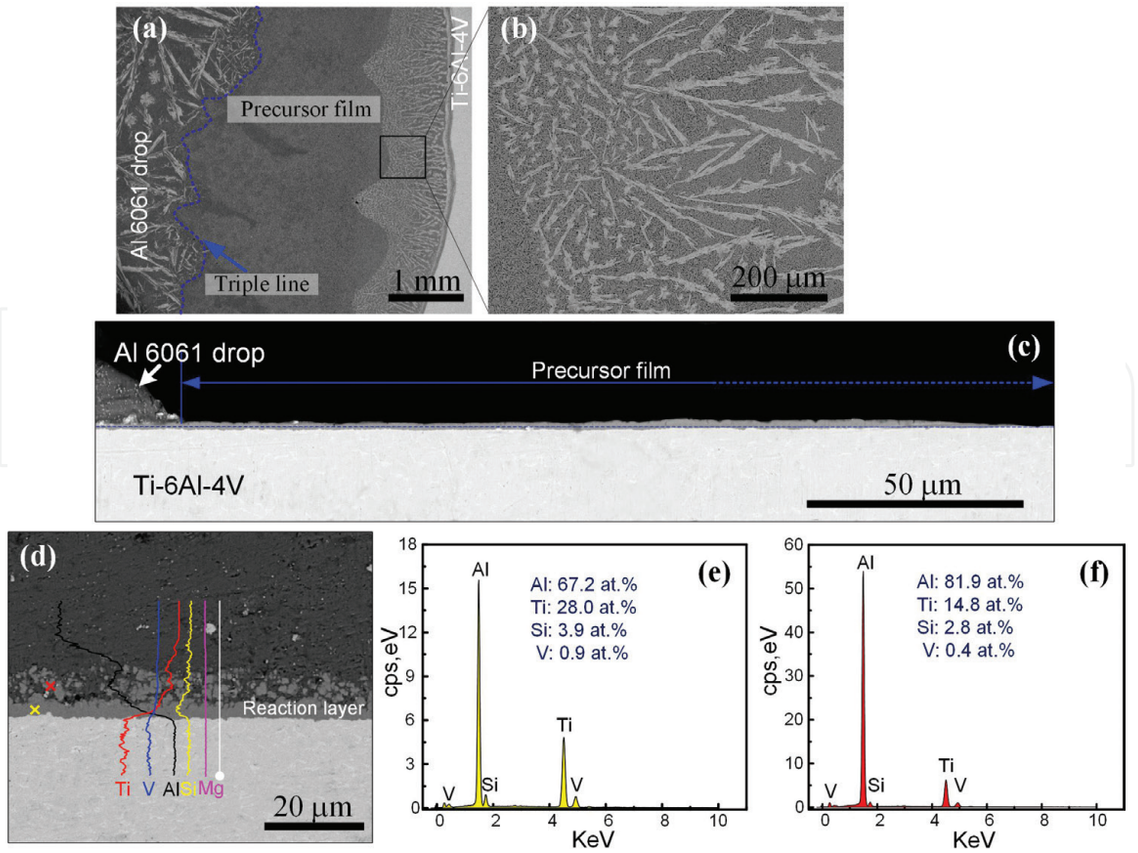

Figure 8.
(a) Top-view of the microstructures around the triple line for Al 6061/TC4 after isothermal wetting at 600°C; (b) detail of the black rectangle area in (a); cross-sectional view of Al 6061/TC4 (c) near the triple line and (d) at central position of the interfacial microstructures with the elemental line distribution results; (e) and (f) EDS results for the corresponding colored crosses in (d), respectively.

alloying elements (Si and Mg) caused the different interfacial structures and are responsible for the different final wettability. In **Figure 8(d)–(f)**, the typical cross-sectional view of Al 6061/TC4 after isothermal wetting at 600°C shows the chemical compositions of the granular phase distributed above the reaction layer are closed to Al_3Ti. The original concentration of Si in the bulk Al 6061 alloys is only 0.6 at.%, but the concentration of Si in the continuous reaction layer is far beyond that value, as shown in **Figure 8(e)**. The distinct segregation of Si in the reaction layer was formed during wetting. For the nonwetting sample of Al 4043/TC4 (after wetting at 600°C), as shown in **Figure 9(a)** and **(b)**, the interfacial structures with the virgate phase but no granular phase near triple line and the virgate phase together with granular phase at the center position can be found. Si concentration in the virgate phase is extremely high comparing with the original concentration in bulk Al 4043 alloy, as shown in **Figures 9(c)–(e)**.

For the wetting sample of Al 4043/TC4 which is similar to the interfacial structures in Al 6061/TC4, a precursor film with width of several millimeters was formed. However, such a precursor film contains two layers, as be shown in **Figure 10(a)** and **(b)**. From the cross-sectional view of the film (**Figure 10(c)**), the upper layer is the residual Al, which was attracted by the capillary force from the loose reaction layer. At the central position of the interface (**Figure 10(d)**), the loose continuous layer also can be found, but the virgate phase almost disappeared and only can be found sporadically above the loose layer. Based on the EDS results (**Figure 10(e)** and **(f)**), the loose layer may be a continuous Al_3Ti layer dissolved with Si as a solid solution. For the sample of Al 4043/TC4 after isothermal wetting at 650°C, the solidified Al was removed by NaOH aqueous solution (1 mol/L), and

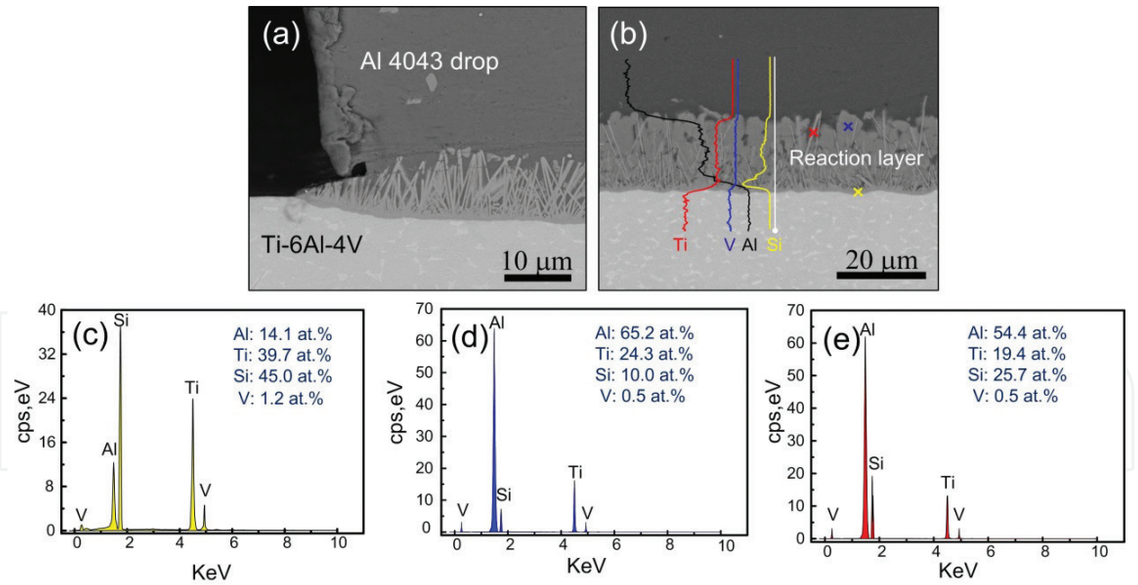

Figure 9.
Cross-sectional views for Al 4043/TC4 after isothermal wetting at 600°C: (a) at the triple line; (b) at the center of the interface; (c)–(e) the EDS results for the corresponding cross, circle and triangle in (b).

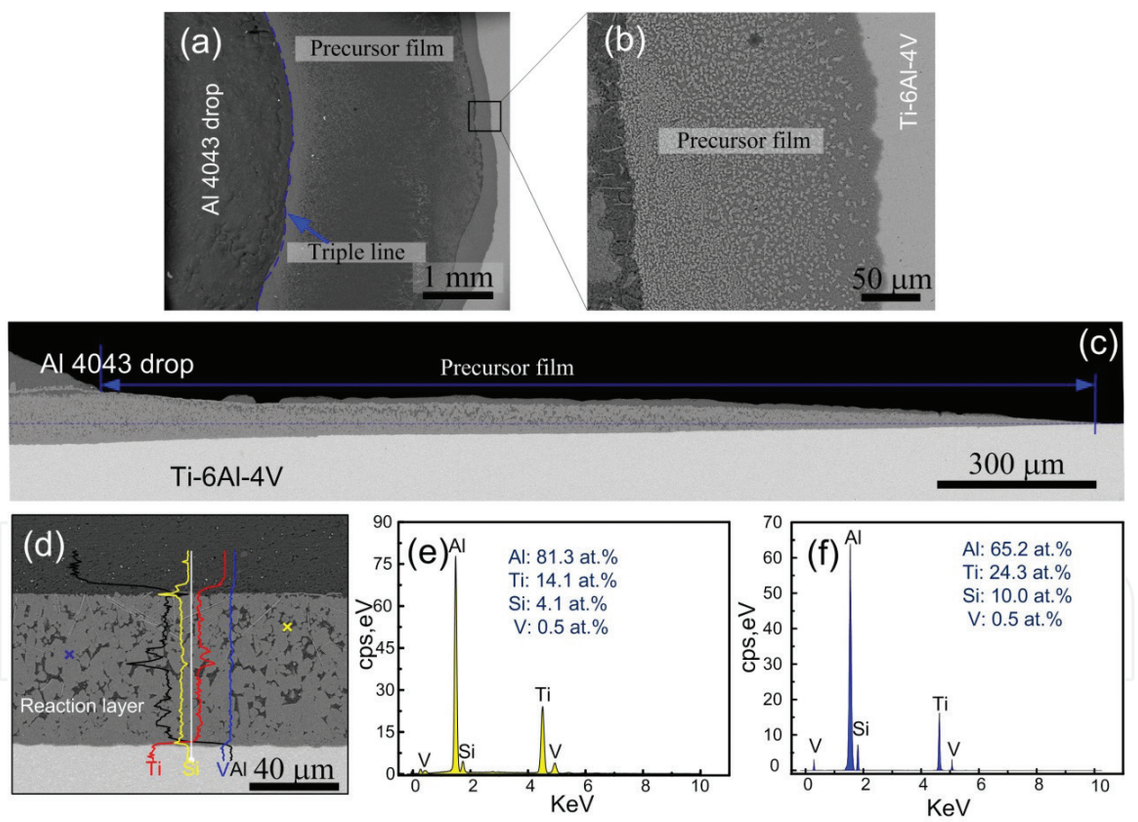

Figure 10.
(a) Top-view of the microstructures at the triple line for Al 4043/TC4 after isothermal wetting at 650°C; (b) detail of the black rectangle area in (a); cross-sectional view of Al 4043/TC4 (c) at the triple line, and (d) at center of the interfacial microstructures with the elemental line distribution results; (e) and (f) EDS results for the corresponding colored crosses in (d), respectively.

the macroscopical appearance of the sample and the details for the corresponding positions were shown in **Figure 11**. The granular phase in **Figure 11(b)** is corresponding to the loose continuous reaction layer, and the lamellate phase is corresponding to virgate phase in the cross-sectional view of the interface. Further, as shown in **Figure 12**, the XRD of the phases at the corresponding surface confirmed

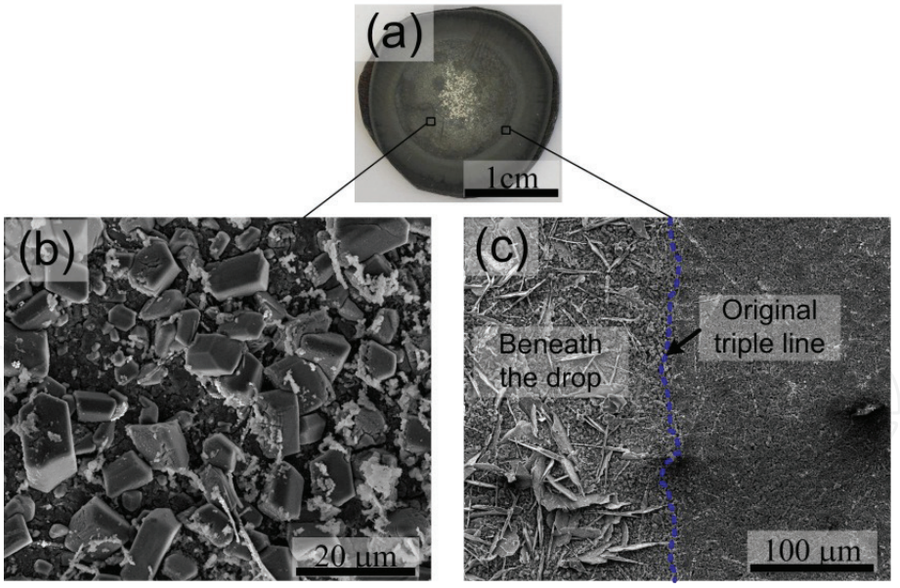

Figure 11.
(a) Solidified Al for the sample of Al 4043/TC4 after isothermal wetting at 650°C was removed by NaOH aqueous solution (1 mol/L); (b) and (c) the microstructures for the corresponding positions in (a).

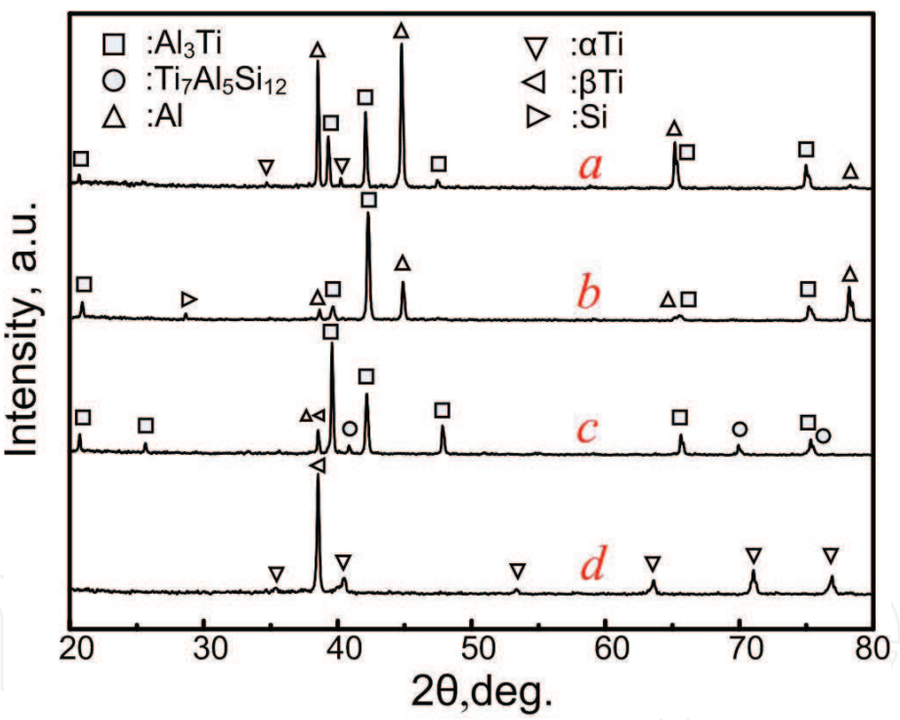

Figure 12.
XRD patterns of the phases at the precursor films: for (a) Al 6061 and (b) Al 4043 samples after isothermal wetting at 700°C; (c) the exposed interface of Al 4043/TC4 after isothermal wetting at 650°C through removing of the solidified Al drop using NaOH aqueous solution, and (d) the original surface of TC4.

the granular phase (the loose continuous reaction layer) is Al_3Ti, and the lamellate phase is $Ti_7Al_5Si_{12}$ (τ_1, a solid solution of Al in the $TiSi_2$ phase [15]).

The formed $Ti_7Al_5Si_{12}$ is a metastable phase, once the temperature was above 579°C, a decomposed reaction of $Ti_7Al_5Si_{12}$ would take place, i.e., $L + \tau_1 \leftrightarrow (Si) + (Al)$, at 579°C [15], where L is the liquid phase in composition (Al: 87.835, Si: 12.1, Ti: 0.065 in at.%), (Al) is in (~98.5 at.% Al and ~1.5 at.% Si). Once the continuous compact $Ti_7Al_5Si_{12}$ layer was formed, the mass transfer at the triple line would be further slowed, and the wettability was improved to a very limited degree (i.e., at 600°C). At higher temperature, $Ti_7Al_5Si_{12}$ was decomposed, and then the formation of Al_3Ti

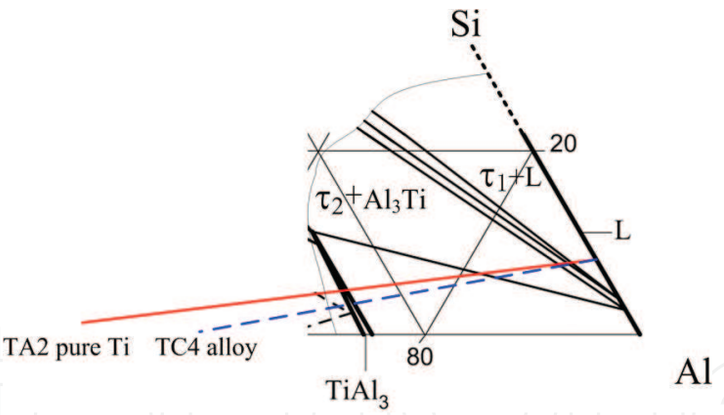

Figure 13.
Al-Ti-Si partial isothermal section at 700°C for Al rich corner [15].

replaced it. Hence, two layers (upper layer is some residual $Ti_7Al_5Si_{12}$, and under layer is Al_3Ti) in the precursor film of Al 6061/TC4 is not surprising, due to lack of L (i.e., the liquid phase) for the decomposed reaction. Also, because of the loosened structures of Al_3Ti, the reaction layer is no longer an obstruction (comparing to $Ti_7Al_5Si1_2$) and the mass transfer was intensified both at the interface and close of triple line, result in wettability was further improved. The interfacial structures of Al 6061/TA2 is similar to that of Al/TC4, so that we do not repeat them here. In this highly reactive wetting system, although the final wettability can be obtained, the interfacial reaction would never stop until the liquid phase was exhausted. Also, the interfacial structures of TA2 and TC4 seems no different, but Al 4043/TC4 alloy system is more incline to obtain Al_3Ti which is in a loosened structure (comparing to $Ti_7Al_5Si_{12}$ layer). As seen in the Al-Ti-Si ternary phase diagram (**Figure 13**) for Al rich corner at 700°C, the path from AlSi5 (i.e., Al 4043) to TC4 alloy (the blue dashed line) is shorter than that from AlSi5 to Ti (red line) as well as the distance of the crossed $\tau_1 + L$ region, which means Al 4043 (Al-5 wt.%Si) alloy contacted with TC4 alloy would induce the formation of Al_3Ti easily. Further, the loosened structure of Al_3Ti layer would cause the more mass transport and better wettability.

Si addition in Al alloys, as known, is a surface-active agent which can decrease the surface tension of the liquid and increase the flowability. However, in Al-Si/steel or Al-Si/Ti system, the interfacial microstructures confirm the affinity of Si to Fe (or Ti) is relatively higher than that of Si to the Al matrix. The Si segregation at the liquid/solid interface satisfies the thermodynamic condition. Such a thermodynamic model also can be used for predicting the segregation of alloying element at the liquid/solid interface. The adsorption energy based on the affinities, which can be described as following [3],

$$E_{M(B)}^{\infty SL} = m_1(\lambda_{AM} - \lambda_{BM} - \lambda_{AB}) \tag{2}$$

where $E_{M(B)}^{\infty SL}$ is adsorption energy, m_1 is an interfacial structure factor (always has a positive value), λ_{ij} is the mole exchange energy for i and j. Here, A, B and M stand for the solid metal, the liquid solvent metal and the solute metal, respectively. The more negative the value of $E_{M(B)}^{\infty SL}$, the solute element is more inclined to segregate at the liquid/solid interface. Further, the positive value of λ_{ij} means two metals is repellent in thermodynamic or weak interaction, or vice versa. We assumed that the binary solution is an infinite dilution regular solution, and λ_{ij} can be calculated from the following [3],

$$\lambda_{ij} = \left(\overline{\Delta H_{i(j)}}^{\infty} + \overline{\Delta H_{j(i)}}^{\infty}\right)/2 \tag{3}$$

where $\overline{\Delta H_{i(j)}}^{\infty}$ and $\overline{\Delta H_{j(i)}}^{\infty}$ represent the mixing enthalpy of i in j and j in i, based on Miedema's model, Ref. [16]. The chemical adsorption is usually considered as a prerequisite for the reaction (or for the precipitation of the reaction product) when the concentration of the adsorbate is below the saturation adsorption concentration. Therefore, $E_{M(B)}^{\infty SL}/m_1$ can be used for the prediction of interfacial structure before experiment.

The calculated $E_{M(B)}^{\infty SL}/m_1$ (−19.8 kJ/mol) has a negative value in Al-Si/Fe system which suggested that Si would segregate at liquid/solid interface and corresponding to some Si segregation in Fe_2Al_5 layer, but the value of $E_{M(B)}^{\infty SL}/m_1$ for the Al-Mg/Fe system is 158.9 kJ/mol. The calculated $E_{M(B)}^{\infty SL}/m_1$ (−73.4 kJ/mol) also has a negative value in the Al-Si/Ti system, but the value of $E_{M(B)}^{\infty SL}/m_1$ for the Al-Mg/Ti system is 221.4 kJ/mol. All the calculated results indicated the segregation at the liquid/solid interface satisfied the thermodynamic model. The E/m_1 for selected systems of the binary solution contacting with a metallic substrate were shown in **Table 3**, of which the segregation at interface or not were verified in our wetting experiments. The positive value of E/m_1 indicates the solute metal would not segregate at solid/liquid interface, and vice versa.

All the variation in spreading of Al/steel and Al/Ti indicated the characteristics of reactive wetting, i.e., the typical linear spreading as well as the interfacial reaction. Reaction-limited models of linear spreading and nonlinear spreading for the description of the wetting behavior, as proposed by Eustathopoulos group, were expressed as following,

$$\frac{dR_d}{dt} = k_1 = C\exp\left(-\frac{\Delta E_a}{RT}\right) \text{ for linear spreading} \quad (4)$$

$$\cos\theta_e - \cos\theta_d = (\cos\theta_e - \cos\theta_0)\exp(-k_2 t) \text{ for nonlinear spreading} \quad (5)$$

where C is a constant which relates to the activity of a reactive solute, ΔE_a is the activation energy for spreading caused by a reaction which may partially contain the activation Gibbs energy of the reaction, R is the gas constant, and T is the temperature in K. The left term dR_d/dt, i.e., the spreading velocity, can be obtained by the linear fitting from **Figure 3(d)**, **(d)** and **(f)** (the slope after fitting, was denoted as k_1). where the θ_0, θ_d, and θ_e, respectively, represent the initial, dynamic, and equilibrium contact angles. k_2 is a kinetic constant which contains the activation energy and can be deduced from the fitting results based on the variations of $\theta - t$ in **Figures 3** and **4**. The logarithms, both of constants k_1 and k_2, were plotted as a function of $1/T$, i.e., the Arrhenius plots, were shown in **Figure 14**. The deduced activation energies from the slopes were shown in **Table 4**.

In Al/steel system, two types of spreading mode, i.e., the linear spreading in Al 4043/steel and nonlinear spreading in Al 6061/steel, can be found. The activation energy for Al 4043/steel can be deduced from the slopes, is 8 kJ/mol for Al 4043. Also, the activation energy for Al 6061 can be deduced from the fitting result of Eq. (5), is 86 kJ/mol. In the work of wetting and spreading of molten pure Al on the surface of mild steel, studied by Ishida [17], the linear kinetics were also observed, and the activation energy is 21.8 kJ/mol. Obviously, the trace elements in the systems influenced the spreading dynamics, and caused the different activation energies. In Al 4043/steel, the segregation of Si at liquid/solid interface enhanced the reactivity, and then might lead to relatively small activation energy. In Al 6061/steel, the liquid Mg in molten Al 6061 alloy does not react with Fe directly. The moving of the triple depends on the removing of oxide film on the surface of substrate. The reduction of Fe—O oxide film by the Mg in Al 6061 and the formation of Fe-Al intermetallics play

B-M/A	Mg-Al/Fe	Mg-Al/Ti	Mg-Zn/Fe	Mg-Si/Fe	Mg-Cu/Fe	Mg-Ni/Fe	Mg-Si/Ti	Mg-Al/Cu	Mg-Si/Cu	Al-Si/Fe
E/m_1 (kJ/mol)	−149	−212	−73	−133	6	−35	−249	−17	21	−20
B-M/A	Al-Zn/Fe	Al-Si/Ti	Al-Si/Cu	Cu-Ag/Si	Ni-Zn/Fe	Al-Cu/Fe	Cu-Si/Fe	Cu-Zn/Fe	Mg-Zn/Ti	Al-Mg/Ti
E/m_1 (kJ/mol)	43	−73	1.8	21	70	181	−118	−42	−137	221

Table 3.
***E/m*$_1$** *of the selected B-M/A systems calculated from Refs. [3, 16].*

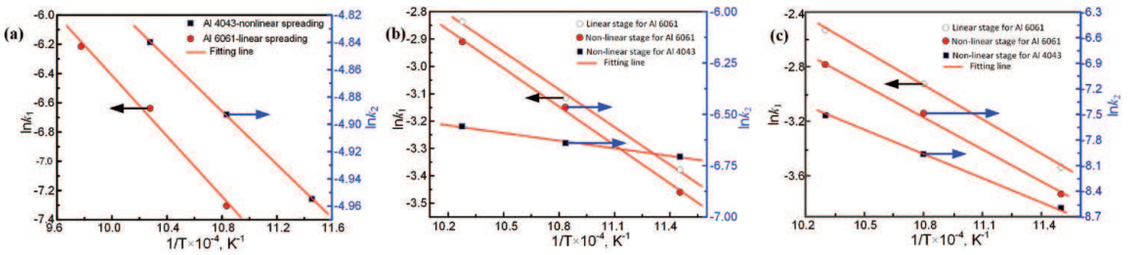

Figure 14.
Arrhenius plot of the kinetic constants k_1 and k_2: (a) Al/steel, (b) Al/TC4 and (c) Al/TA2.

Systems	Al6061/steel	Al4043/steel	Al6061/TC4*	Al4043/TC4	Al6061/TA2*	Al4043/TA2
E_a (kJ/mol)	86	8	50	10	84	47

**The average activation energy of linear stage and nonlinear stage.*

Table 4.
Deduced activation energies from the slopes in **Figure 14.**

a combined action in the removing of oxide film, which can induce the spreading. Two spreading stages for Al 6061 at 700°C also indicate these two reaction mechanisms. Especially for the latter stage, the reduction reaction mechanism may play a major role on the moving of the triple line corresponding to the prolonged precursor film in this stage. Therefore, the apparent activation energy in Al 6061 is so different from Al 4043 and almost an order of magnitude larger.

In Al/TC4 system, such apparent activation energies should relate to the energy change of reaction. As suggested by Chen et al. [18], Gibbs energy changes of reaction per mole of reactants for the formation of $Ti_7Al_5Si_{12}$ and Al_3Ti in the range of 600–750°C are ~− 48 kJ/mol and ~− 30 kJ/mol, respectively. For the nonlinear stage, $Ti_7Al_5Si_{12}$ decomposition may play a dominant role in the change of interface tension corresponding to the apparent activation energy of 10–38 kJ/mol; for the linear stage, the decomposition of $Ti_7Al_5Si_{12}$ and the formation of Al_3Ti may play the role for the change of interface tension corresponding to the apparent activation energy of 62 kJ/mol. The relatively higher activity of Si in Al 4043 (due to the higher concentration) may slow down the decomposition of $Ti_7Al_5Si_{12}$, and then decrease the apparent activation energy. Further, the residual $Ti_7Al_5Si_{12}$ beneath the drop and above on Al_3Ti reaction layer at the close of the triple line (**Figure 11(c)**) should be one of the indicators that two reaction mechanisms together played a role on change of interface tension. Also, in Al/TA2 system, the apparent activation energies indicated that the whole wetting process is controlled by the above mechanism. Therefore, the activation energies (47–84 kJ/mol) may be also corresponding to the decomposition of $Ti_7Al_5Si_{12}$ and the formation of Al_3Ti.

4. Conclusions

Aluminizing of steel or Ti alloys can increase the ability of anti-corrosion, the service time and the working temperature, significantly. The wetting of Al alloys plays an important role in the aluminizing process, and thus studied in this work. The following conclusions can be drawn:

1. In Al/steel, the wettability was improved by intermetallic formation which would lead to the replacement of the oxidized surface by a clean surface of

an intermetallic compound, also due to the reduction by Al with oxide film; However, the final wettability of pure Ti (TA2) and Ti alloys (TC4) by Al was less affected by the oxide film, but was determined by the reaction products at the liquid/solid interface. Enhanced peritectic reaction of $Ti_7Al_5Si_{12}$ caused the different interfacial structures of TA2 and TC4.

2. The alloying elements in Al 6061 alloy (with Mg addition) and Al 4043 alloy (with Si addition) resulted in distinctly different interfacial structures, the formation of precursor film and spreading dynamics. Mg played a role like gas flux and reduced the oxide film on the surface of substrate. Si segregated at solid/liquid interface which satisfied the thermodynamic model. Such a thermodynamic model also can be used for predicting the element segregation at the interface.

3. The precursor film in these reactive wetting systems is an extended reaction layer. The formation of it satisfies subcutaneous infiltration mechanism.

4. The spreading dynamics of these systems can be described by RPC model, and the activation energies are related to the removing of oxide film covered the substrate or the reaction at interface.

Acknowledgements

This work is supported by National Natural Science Foundation of China (no. 51665031), "Kaiwu" Innovation Team Support Project of Lanzhou Institute of Technology (no. 2018KW-05).

Conflict of interest

We have no conflicts of interest to declare.

Author details

Qiaoli Lin[1*], Ran Sui[2] and Weiyuan Yu[1]

1 State Key Laboratory of Advanced Processing and Recycling of Non-ferrous Metal, Lanzhou University of Technology, Lanzhou, People's Republic of China

2 Department of Materials Science and Engineering, Lanzhou Institute of Technology, Lanzhou, People's Republic of China

*Address all correspondence to: lqllinqiaoli@163.com

References

[1] Young T. An essay on the cohesion of fluids. Philosophical Transactions of the Royal Society of London. 1805;**95**:65-87. DOI: 10.1098/rstl.1805.0005

[2] Yong-Taeg O, Fujino S, Morinaga K. Fabrication of transparent silica glass by powder sintering. Science and Technology of Advanced Materials. 2002;**3**:297-301. DOI: 10.1016/s1468-6996 (02)00030-x

[3] Eustathopoulos N, Nicholas MG, Drevet B. Wettability at High Temperatures. Oxford: Elsevier; 1999. 106 p

[4] Lin Q, Qiu F, Sui R. Characteristics of precursor film in the wetting of Zr-based alloys on ZrC substrate at 1253 K. Thin Solid Films. 2014;**558**: 231-236. DOI: 10.1016/j.tsf.2014.02.074

[5] Be'er A, Lereah Y, Taitelbaum H. Reactive wetting of Hg-Ag system at room temperature. Materials Science and Engineering: A. 2008;**495**:102-107. DOI: 10.1016/j.msea.2007.11.095

[6] de Gennes PG. Wetting: Statics and dynamics. Reviews of Modern Physics. 1985;**57**:827. DOI: 10.1103/RevModPhys.57.827

[7] Li ZK, Ma GF, Fu HM, Sha PF, Zhang B, Zhu ZW, et al. The spreading kinetics and precursor film characteristics of Zr-based alloy melt on W substrate. Materials Letters. 2013;**98**:98-101. DOI: 10.1016/j.matlet.2013.02.005

[8] Lemmens B, Gonzalez Garcia Y, Corlu B, De Strycker J, De Graeve I, Verbeken K. Study of the electrochemical behaviour of aluminized steel. Surface and Coatings Technology. 2014;**260**:34-38. DOI: /10.1016/j.surfcoat.2014.06.064

[9] Gupta SP. Intermetallic compound formation in Fe–Al–Si ternary system: Part I. Materials Characterization. 2002;**49**:269-291. DOI: 10.1016/S1044-5803(03)00006-8

[10] Protsenko P, Terlain A, Traskine V, Eustathopoulos N. The role of intermetallics in wetting in metallic systems. Scripta Materialia. 2001;**45**:1439-1445. DOI: 10.1016/S1359-6462(01)01181-2

[11] Durandet YC, Strezov L, Ebrill N. Formation of Al-Zn-Si coatings on low carbon steel substrates. In: Proceedings of the 4th International Conference on Zinc and Zinc Alloys Coated Steel Sheet (GALVATECH '98). Chiba: The Iron and Steel Institute of Japan; 1998. pp. 147-151

[12] Barin I. Thermochemical Data of Pure Substances. 3rd ed. Weinheim: Wiley-VCH Verlag GmbH; 1995. 702 p

[13] Miller CJ, Pa P. Fluxless aluminum brazing. US Patent: 3373483; 1968

[14] Zhuang H, Lugscheider E. High Temperature Brazing. Beijing: National Defense Industry Press; 1989. 158 p

[15] Perrot P. Aluminum—silico n-titanium. In: Effenberg G, Ilyenko S, editors. Light Metal Systems, Part 4: Selected Systems from Al-Si-Ti to Ni-Si-Ti. Berlin-Heidelberg: Springer-Verlag; 2006. pp. 1-15. DOI: 10.1007/11008514_2

[16] Zhang RF, Sheng SH, Liu BX. Predicting the formation enthalpies of binary intermetallic compounds. Chemical Physics Letters. 2007;**442**: 511-514. DOI: 10.1016/j.cplett.2007.06.031

[17] Ishida T. Spreading kinetics of liquid metals on mild steel. Journal Materials Science and Technolog. 1988;**4**:830-835. DOI: 10.1179/mst.1988.4.9.830

[18] Chen S, Li L, Chen,Y, Liu D. Si diffusion behavior during laser weldingbrazing of Al alloy and Ti alloy with Al-12Si filler wire. Transactions of Nonferrous Metals Society of China. 2010;**20**:64-70. DOI: 10.1016/S1003-6326(09)60098-4